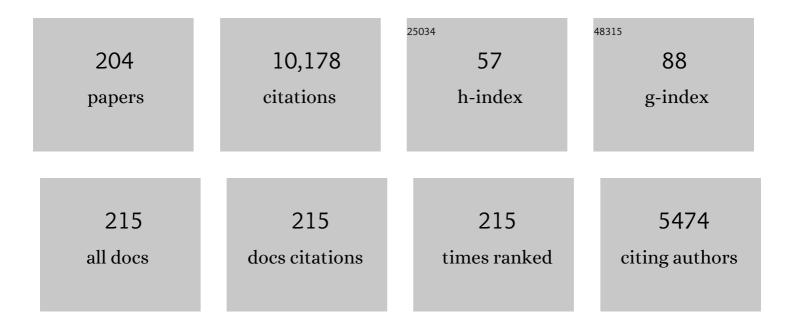
Douglas A Wiens

List of Publications by Year in descending order

Source: https://exaly.com/author-pdf/4870495/publications.pdf Version: 2024-02-01



#	Article	IF	CITATIONS
1	The seismic structure of the Antarctic upper mantle. Geological Society Memoir, 2023, 56, 195-212.	1.7	15
2	Antarctic upper mantle rheology. Geological Society Memoir, 2023, 56, 267-294.	1.7	14
3	Lithospheric Erosion in the Patagonian Slab Window, and Implications for Glacial Isostasy. Geophysical Research Letters, 2022, 49, .	4.0	12
4	Radial Anisotropy and Sediment Thickness of West and Central Antarctica Estimated From Rayleigh and Love Wave Velocities. Journal of Geophysical Research: Solid Earth, 2022, 127, .	3.4	7
5	Shear Wave Splitting Across Antarctica: Implications for Upper Mantle Seismic Anisotropy. Journal of Geophysical Research: Solid Earth, 2022, 127, .	3.4	3
6	Teleseismic earthquake wavefields observed on the Ross Ice Shelf. Journal of Glaciology, 2021, 67, 58-74.	2.2	4
7	Seismicity and Pn Velocity Structure of Central West Antarctica. Geochemistry, Geophysics, Geosystems, 2021, 22, e2020GC009471.	2.5	7
8	Swell-Triggered Seismicity at the Near-Front Damage Zone of the Ross Ice Shelf. Seismological Research Letters, 2021, 92, 2768-2792.	1.9	14
9	Diamonds Hold Clues About the Cause of Deep Earthquakes. AGU Advances, 2021, 2, e2021AV000434.	5.4	2
10	Upper Mantle Hydration Indicated by Decreased Shear Velocity Near the Southern Mariana Trench From Rayleigh Wave Tomography. Geophysical Research Letters, 2021, 48, e2021GL093309.	4.0	17
11	Seismic Structure of the Antarctic Upper Mantle Imaged with Adjoint Tomography. Journal of Geophysical Research: Solid Earth, 2020, 125, .	3.4	59
12	The Alaska Amphibious Community Seismic Experiment. Seismological Research Letters, 2020, 91, 3054-3063.	1.9	28
13	A joint inversion of receiver function and Rayleigh wave phase velocity dispersion data to estimate crustal structure in West Antarctica. Geophysical Journal International, 2020, 223, 1644-1657.	2.4	11
14	Prominent thermal anomalies in the mantle transition zone beneath the Transantarctic Mountains. Geology, 2020, 48, 748-752.	4.4	5
15	A Geothermal Heat Flux Map of Antarctica Empirically Constrained by Seismic Structure. Geophysical Research Letters, 2020, 47, e2020GL086955.	4.0	51
16	High Rates of Deep Earthquake Dynamic Triggering in the Thermal Halos of Subducting Slabs. Geophysical Research Letters, 2020, 47, e2019GL086125.	4.0	6
17	Seismicity of the Incoming Plate and Forearc Near the Mariana Trench Recorded by Ocean Bottom Seismographs. Geochemistry, Geophysics, Geosystems, 2020, 21, e2020GC008953.	2.5	12
18	P- and S-wave velocity structure of central West Antarctica: Implications for the tectonic evolution of the West Antarctic Rift System. Earth and Planetary Science Letters, 2020, 546, 116437.	4.4	15

#	Article	IF	CITATIONS
19	High Bulk and Shear Attenuation Due to Partial Melt in the Tonga‣au Backâ€arc Mantle. Journal of Geophysical Research: Solid Earth, 2020, 125, e2019JB017527.	3.4	19
20	Glacial Earthquakes and Precursory Seismicity Associated With Thwaites Glacier Calving. Geophysical Research Letters, 2020, 47, e2019GL086178.	4.0	12
21	Crustal and lithospheric structure of inactive volcanic arc terrains in Fiji. Tectonophysics, 2019, 750, 394-403.	2.2	6
22	Ross Ice Shelf Icequakes Associated With Ocean Gravity Wave Activity. Geophysical Research Letters, 2019, 46, 8893-8902.	4.0	25
23	The uppermost mantle seismic velocity structure of West Antarctica from Rayleigh wave tomography: Insights into tectonic structure and geothermal heat flow. Earth and Planetary Science Letters, 2019, 522, 219-233.	4.4	18
24	Mapping Crustal Shear Wave Velocity Structure and Radial Anisotropy Beneath West Antarctica Using Seismic Ambient Noise. Geochemistry, Geophysics, Geosystems, 2019, 20, 5014-5037.	2.5	10
25	Seasonal and spatial variations in the ocean-coupled ambient wavefield of the Ross Ice Shelf. Journal of Glaciology, 2019, 65, 912-925.	2.2	12
26	Solid Earth change and the evolution of the Antarctic Ice Sheet. Nature Communications, 2019, 10, 503.	12.8	93
27	Tidal and Thermal Stresses Drive Seismicity Along a Major Ross Ice Shelf Rift. Geophysical Research Letters, 2019, 46, 6644-6652.	4.0	29
28	<i>P</i> Wave Teleseismic Traveltime Tomography of the North American Midcontinent. Journal of Geophysical Research: Solid Earth, 2019, 124, 1725-1742.	3.4	15
29	Intermediateâ€Depth Earthquakes Controlled by Incoming Plate Hydration Along Bendingâ€Related Faults. Geophysical Research Letters, 2019, 46, 3688-3697.	4.0	30
30	Complex and Diverse Rupture Processes of the 2018Mw8.2 andMw7.9 Tongaâ€Fiji Deep Earthquakes. Geophysical Research Letters, 2019, 46, 2434-2448.	4.0	14
31	Heterogeneous upper mantle structure beneath the Ross Sea Embayment and Marie Byrd Land, West Antarctica, revealed by P-wave tomography. Earth and Planetary Science Letters, 2019, 513, 40-50.	4.4	23
32	Seismic evidence for lithospheric foundering beneath the southern Transantarctic Mountains, Antarctica. Geology, 2018, 46, 71-74.	4.4	44
33	Water input into the Mariana subduction zone estimated from ocean-bottom seismic data. Nature, 2018, 563, 389-392.	27.8	141
34	Ocean-excited plate waves in the Ross and Pine Island Glacier ice shelves. Journal of Glaciology, 2018, 64, 730-744.	2.2	15
35	Nearâ€ S urface Environmentally Forced Changes in the Ross Ice Shelf Observed With Ambient Seismic Noise. Geophysical Research Letters, 2018, 45, 11,187.	4.0	21
36	P-wave attenuation structure of the Lau back-arc basin and implications for mantle wedge processes. Earth and Planetary Science Letters, 2018, 502, 187-199.	4.4	27

#	Article	IF	CITATIONS
37	The Crust and Upper Mantle Structure of Central and West Antarctica From Bayesian Inversion of Rayleigh Wave and Receiver Functions. Journal of Geophysical Research: Solid Earth, 2018, 123, 7824-7849.	3.4	78
38	Reactivation of ancient Antarctic rift zones by intraplate seismicity. Nature Geoscience, 2018, 11, 515-519.	12.9	24
39	Observed rapid bedrock uplift in Amundsen Sea Embayment promotes ice-sheet stability. Science, 2018, 360, 1335-1339.	12.6	147
40	Slab temperature controls on the Tonga double seismic zone and slab mantle dehydration. Science Advances, 2017, 3, e1601755.	10.3	48
41	Tsunami and infragravity waves impacting <scp>A</scp> ntarctic ice shelves. Journal of Geophysical Research: Oceans, 2017, 122, 5786-5801.	2.6	35
42	The uppermost mantle seismic velocity and viscosity structure of central West Antarctica. Earth and Planetary Science Letters, 2017, 472, 38-49.	4.4	29
43	Sea Level Fingerprints in a Region of Complex Earth Structure: The Case of WAIS. Journal of Climate, 2017, 30, 1881-1892.	3.2	44
44	Implications of Sea Ice on Southern Ocean Microseisms Detected by a Seismic Array in West Antarctica. Geophysical Journal International, 2017, , ggx007.	2.4	6
45	Influence of a West Antarctic mantle plume on ice sheet basal conditions. Journal of Geophysical Research: Solid Earth, 2017, 122, 7127-7155.	3.4	57
46	Crustal structure of the Transantarctic Mountains, Ellsworth Mountains and Marie Byrd Land, Antarctica: constraints on shear wave velocities, Poisson's ratios and Moho depths. Geophysical Journal International, 2017, 211, 1328-1340.	2.4	23
47	Shear velocity structure of the crust and upper mantle of Madagascar derived from surface wave tomography. Earth and Planetary Science Letters, 2017, 458, 405-417.	4.4	40
48	Upper mantle shear wave velocity structure beneath northern Victoria Land, Antarctica: Volcanism and uplift in the northern Transantarctic Mountains. Earth and Planetary Science Letters, 2016, 449, 48-60.	4.4	23
49	Dynamic triggering of deep earthquakes within a fossil slab. Geophysical Research Letters, 2016, 43, 9492-9499.	4.0	12
50	Upper mantle structure of the <scp>T</scp> ongaâ€ <scp>L</scp> auâ€ <scp>F</scp> iji region from <scp>R</scp> ayleigh wave tomography. Geochemistry, Geophysics, Geosystems, 2016, 17, 4705-4724.	2.5	15
51	Distinct crustal structure of the North American Midcontinent Rift from <i>P</i> wave receiver functions. Journal of Geophysical Research: Solid Earth, 2016, 121, 8136-8153.	3.4	32
52	Upper mantle structure of central and West Antarctica from array analysis of Rayleigh wave phase velocities. Journal of Geophysical Research: Solid Earth, 2016, 121, 1758-1775.	3.4	84
53	Crustal and upper-mantle structure beneath ice-covered regions in Antarctica from <i>S</i> -wave receiver functions and implications for heat flow. Geophysical Journal International, 2016, 204, 1636-1648.	2.4	36
54	Strong seismic scatterers near the core–mantle boundary north of the Pacific Anomaly. Physics of the Earth and Planetary Interiors, 2016, 253, 21-30.	1.9	16

#	Article	IF	CITATIONS
55	Ice shelf structure derived from dispersion curve analysis of ambient seismic noise, Ross Ice Shelf, Antarctica. Geophysical Journal International, 2016, 205, 785-795.	2.4	40
56	Temperature, lithosphereâ€asthenosphere boundary, and heat flux beneath the Antarctic Plate inferred from seismic velocities. Journal of Geophysical Research: Solid Earth, 2015, 120, 8720-8742.	3.4	129
57	A seismic transect across West Antarctica: Evidence for mantle thermal anomalies beneath the Bentley Subglacial Trench and the Marie Byrd Land Dome. Journal of Geophysical Research: Solid Earth, 2015, 120, 8439-8460.	3.4	54
58	The 3 May 2006 (<i>M_w</i> 8.0) and 19 March 2009 (<i>M_w</i> 7.6) Tonga earthquakes: Intraslab compressional faulting below the megathrust. Journal of Geophysical Research: Solid Earth, 2015, 120, 6297-6316.	3.4	11
59	Ross ice shelf vibrations. Geophysical Research Letters, 2015, 42, 7589-7597.	4.0	52
60	The mantle transition zone beneath <scp>W</scp> est <scp>A</scp> ntarctica: Seismic evidence for hydration and thermal upwellings. Geochemistry, Geophysics, Geosystems, 2015, 16, 40-58.	2.5	38
61	<i>P</i> and <i>S</i> velocity tomography of the Mariana subduction system from a combined land-sea seismic deployment. Geochemistry, Geophysics, Geosystems, 2015, 16, 681-704.	2.5	29
62	Lithospheric instability and the source of the Cameroon Volcanic Line: Evidence from Rayleigh wave phase velocity tomography. Journal of Geophysical Research: Solid Earth, 2015, 120, 1708-1727.	3.4	42
63	A previously unreported type of seismic source in the firn layer of the East Antarctic Ice Sheet. Journal of Geophysical Research F: Earth Surface, 2015, 120, 2237-2252.	2.8	14
64	Seasonal and Diurnal Variations in Longâ€Period Noise at SPREE Stations: The Influence of Soil Characteristics on Shallow Stations' Performance. Bulletin of the Seismological Society of America, 2015, 105, 2433-2452.	2.3	45
65	Seismic evidence of effects of water on melt transport in the Lau back-arc mantle. Nature, 2015, 518, 395-398.	27.8	39
66	Incoming plate faulting in the Northern and Western Pacific and implications for subduction zone water budgets. Earth and Planetary Science Letters, 2015, 414, 176-186.	4.4	36
67	The Seismic Noise Environment of Antarctica. Seismological Research Letters, 2015, 86, 431-431.	1.9	1
68	The Seismic Noise Environment of Antarctica. Seismological Research Letters, 2015, 86, 89-100.	1.9	50
69	Antarctic ice velocities from GPS locations logged by seismic stations. Antarctic Science, 2015, 27, 210-222.	0.9	4
70	<i>S</i> â€velocity model and inferred Moho topography beneath the Antarctic Plate from Rayleigh waves. Journal of Geophysical Research: Solid Earth, 2015, 120, 359-383.	3.4	139
71	Eruption of South Sarigan Seamount, Northern Mariana Islands: Insights into Hazards from Submarine Volcanic Eruptions. Oceanography, 2014, 27, 24-31.	1.0	15
72	The crustal thickness of West Antarctica. Journal of Geophysical Research: Solid Earth, 2014, 119, 378-395.	3.4	103

#	Article	IF	CITATIONS
73	Evidence for bathymetric control on the distribution of body wave microseism sources from temporary seismic arrays in Africa. Geophysical Journal International, 2014, 197, 1869-1883.	2.4	29
74	Upper mantle seismic anisotropy beneath the West Antarctic Rift System and surrounding region from shear wave splitting analysis. Geophysical Journal International, 2014, 198, 414-429.	2.4	27
75	Seismological imaging of ridge–arc interaction beneath the Eastern Lau Spreading Center from OBS ambient noise tomography. Earth and Planetary Science Letters, 2014, 408, 194-206.	4.4	25
76	Imaging the Antarctic mantle using adaptively parameterized P-wave tomography: Evidence for heterogeneous structure beneath West Antarctica. Earth and Planetary Science Letters, 2014, 408, 66-78.	4.4	76
77	Antarctic icequakes triggered by the 2010 Maule earthquake in Chile. Nature Geoscience, 2014, 7, 677-681.	12.9	44
78	Reconciling mantle attenuation-temperature relationships from seismology, petrology, and laboratory measurements. Geochemistry, Geophysics, Geosystems, 2014, 15, 3521-3542.	2.5	71
79	Seismic and geodetic evidence for groundingâ€line control of Whillans Ice Stream stickâ€slip events. Journal of Geophysical Research F: Earth Surface, 2014, 119, 333-348.	2.8	55
80	Faulting within the Pacific plate at the Mariana Trench: Implications for plate interface coupling and subduction of hydrous minerals. Journal of Geophysical Research: Solid Earth, 2014, 119, 3076-3095.	3.4	38
81	Tidal pacing, skipped slips and the slowdown of Whillans Ice Stream, Antarctica. Journal of Glaciology, 2014, 60, 795-807.	2.2	81
82	Broadband seismic deployments in East Antarctica: IPY contribution to monitoring the Earth's interiors. Annals of Geophysics, 2014, 57, .	1.0	3
83	Rayleigh wave constraints on the structure and tectonic history of the Gamburtsev Subglacial Mountains, East Antarctica. Journal of Geophysical Research: Solid Earth, 2013, 118, 2138-2153.	3.4	50
84	Upper mantle seismic structure beneath central East Antarctica from body wave tomography: Implications for the origin of the Gamburtsev Subglacial Mountains. Geochemistry, Geophysics, Geosystems, 2013, 14, 902-920.	2.5	25
85	Seismic detection of an active subglacial magmatic complex in Marie Byrd Land, Antarctica. Nature Geoscience, 2013, 6, 1031-1035.	12.9	55
86	Improving Models of Earth's Response to Ice and Ocean Loading Changes. Eos, 2013, 94, 353-353.	0.1	0
87	Nucleation and seismic tremor associated with the glacial earthquakes of Whillans Ice Stream, Antarctica. Geophysical Research Letters, 2013, 40, 312-315.	4.0	71
88	The relationship of intermediate- and deep-focus seismicity to the hydration and dehydration of subducting slabs. Earth and Planetary Science Letters, 2012, 349-350, 153-160.	4.4	36
89	Motion of an Antarctic glacier by repeated tidally modulated earthquakes. Nature Geoscience, 2012, 5, 623-626.	12.9	66
90	Crustal structure from the Lützow-Holm Bay to the inland plateau of East Antarctica, based on onshore gravity surveys and broadband seismic deployments. Tectonophysics, 2012, 572-573, 100-110.	2.2	3

#	Article	IF	CITATIONS
91	Comparison of global synthetic seismograms calculated using the spherical 2.5-D finite-difference method with observed long-period waveforms including data from the intra-Antarctic region. Polar Science, 2012, 6, 155-164.	1.2	5
92	Upper-mantle anisotropy beneath the Cameroon Volcanic Line and Congo Craton from shear wave splitting measurements. Geophysical Journal International, 2012, 190, 75-86.	2.4	35
93	Seismogenic characteristics of the Northern Mariana shallow thrust zone from local array data. Geochemistry, Geophysics, Geosystems, 2011, 12, n/a-n/a.	2.5	14
94	Shallow seismicity and tectonics of the central and northern Lau Basin. Earth and Planetary Science Letters, 2011, 304, 538-546.	4.4	21
95	Dynamics of stick–slip motion, Whillans Ice Stream, Antarctica. Earth and Planetary Science Letters, 2011, 305, 283-289.	4.4	60
96	Crustal Vp-Vs ratios and thickness for Ross Island and the Transantarctic Mountain front, Antarctica. Geophysical Journal International, 2011, 185, 85-92.	2.4	26
97	Mantle transition zone thickness beneath Cameroon: evidence for an upper mantle origin for the Cameroon Volcanic Line. Geophysical Journal International, 2011, 187, 1146-1150.	2.4	54
98	Learning from failure: The SPREE Mid-Continent Rift Experiment. GSA Today, 2011, 21, 5-7.	2.0	19
99	Structure of the crust beneath Cameroon, West Africa, from the joint inversion of Rayleigh wave group velocities and receiver functions. Geophysical Journal International, 2010, 183, 1061-1076.	2.4	130
100	Shear velocity structure of the Mariana mantle wedge from Rayleigh wave phase velocities. Journal of Geophysical Research, 2010, 115, .	3.3	14
101	Crustal structure of the Transantarctic Mountains near the Ross Sea from ambient seismic noise tomography. Journal of Geophysical Research, 2010, 115, .	3.3	22
102	Upper mantle structure beneath Cameroon from body wave tomography and the origin of the Cameroon Volcanic Line. Geochemistry, Geophysics, Geosystems, 2010, 11, .	2.5	90
103	Crustal structure of the Gamburtsev Mountains, East Antarctica, from S-wave receiver functions and Rayleigh wave phase velocities. Earth and Planetary Science Letters, 2010, 300, 395-401.	4.4	74
104	Upper mantle seismic anisotropy of South Victoria Land and the Ross Sea coast, Antarctica from SKS and SKKS splitting analysis. Geophysical Journal International, 2009, 178, 729-741.	2.4	21
105	Seismic attenuation tomography of the Mariana subduction system: Implications for thermal structure, volatile distribution, and slow spreading dynamics. Geochemistry, Geophysics, Geosystems, 2009, 10, .	2.5	82
106	Using S wave receiver functions to estimate crustal structure beneath ice sheets: An application to the Transantarctic Mountains and East Antarctic craton. Geochemistry, Geophysics, Geosystems, 2009, 10, .	2.5	49
107	Performance Characteristics of a Rotational Seismometer for Near-Field and Engineering Applications. Bulletin of the Seismological Society of America, 2009, 99, 1181-1189.	2.3	20
108	Simultaneous teleseismic and geodetic observations of the stick–slip motion of an Antarctic ice stream. Nature, 2008, 453, 770-774.	27.8	141

#	Article	IF	CITATIONS
109	The Seismic Structure and Dynamics of the Mantle Wedge. Annual Review of Earth and Planetary Sciences, 2008, 36, 421-455.	11.0	114
110	Earthquake evidence for alongâ€arc extension in the Mariana Islands. Geochemistry, Geophysics, Geosystems, 2008, 9, .	2.5	22
111	Mantle transition zone thickness beneath Ross Island, the Transantarctic Mountains, and East Antarctica. Geophysical Research Letters, 2008, 35, .	4.0	15
112	Seismic evidence for widespread serpentinized forearc mantle along the Mariana convergence margin. Geophysical Research Letters, 2008, 35, .	4.0	47
113	Rapid mantle flow beneath the Tonga volcanic arc. Earth and Planetary Science Letters, 2007, 264, 299-307.	4.4	49
114	Double seismic discontinuities at the base of the mantle transition zone near the Mariana slab. Geophysical Research Letters, 2007, 34, .	4.0	16
115	Complex mantle flow in the Mariana subduction system: evidence from shear wave splitting. Geophysical Journal International, 2007, 170, 371-386.	2.4	81
116	Seismic structure beneath the Tonga arc and Lau back-arc basin determined from joint Vp, Vp/Vs tomography. Geochemistry, Geophysics, Geosystems, 2006, 7, n/a-n/a.	2.5	65
117	P and S velocity structure of the upper mantle beneath the Transantarctic Mountains, East Antarctic craton, and Ross Sea from travel time tomography. Geochemistry, Geophysics, Geosystems, 2006, 7, n/a-n/a.	2.5	61
118	Upper mantle thermal variations beneath the Transantarctic Mountains inferred from teleseismic S-wave attenuation. Geophysical Research Letters, 2006, 33, .	4.0	36
119	Depth of the 660-km discontinuity near the Mariana slab from an array of ocean bottom seismographs. Geophysical Research Letters, 2006, 33, .	4.0	12
120	Rayleigh wave phase velocity analysis of the Ross Sea, Transantarctic Mountains, and East Antarctica from a temporary seismograph array. Journal of Geophysical Research, 2006, 111, n/a-n/a.	3.3	55
121	Crust and upper mantle structure of the Transantarctic Mountains and surrounding regions from receiver functions, surface waves, and gravity: Implications for uplift models. Geochemistry, Geophysics, Geosystems, 2006, 7, n/a-n/a.	2.5	73
122	Mantle structure and flow patterns beneath active back-arc basins inferred from passive seismic and electromagnetic methods. Geophysical Monograph Series, 2006, , 43-62.	0.1	3
123	Mantle temperature variations beneath back-arc spreading centers inferred from seismology, petrology, and bathymetry. Earth and Planetary Science Letters, 2006, 248, 30-42.	4.4	80
124	Long-term eruptive activity at a submarine arc volcano. Nature, 2006, 441, 494-497.	27.8	141
125	Seismicity and tilt associated with the 2003 Anatahan eruption sequence. Journal of Volcanology and Geothermal Research, 2005, 146, 60-76.	2.1	21
126	Crustal and upper mantle S-wave velocity structure beneath the Bransfield Strait (West Antarctica) from regional surface wave tomography. Tectonophysics, 2005, 397, 241-259.	2.2	30

#	Article	IF	CITATIONS
127	Detailed structure and sharpness of upper mantle discontinuities in the Tonga subduction zone from regional broadband arrays. Journal of Geophysical Research, 2005, 110, .	3.3	28
128	Tilt recorded by a portable broadband seismograph: The 2003 eruption of Anatahan Volcano, Mariana Islands. Geophysical Research Letters, 2005, 32, n/a-n/a.	4.0	35
129	Observing the historic eruption of northern Mariana Islands volcano. Eos, 2004, 85, 2.	0.1	3
130	Combined Receiver-Function and Surface Wave Phase-Velocity Inversion Using a Niching Genetic Algorithm: Application to Patagonia. Bulletin of the Seismological Society of America, 2004, 94, 977-987.	2.3	69
131	Remote triggering of deep earthquakes in the 2002 Tonga sequences. Nature, 2003, 424, 921-925.	27.8	63
132	Tonga Ridge and Lau Basin crustal structure from seismic refraction data. Journal of Geophysical Research, 2003, 108, .	3.3	93
133	Crustal and upper mantle structure of southernmost South America inferred from regional waveform inversion. Journal of Geophysical Research, 2003, 108, .	3.3	22
134	Source characteristics of large deep earthquakes: Constraint on the faulting mechanism at great depths. Journal of Geophysical Research, 2003, 108, .	3.3	48
135	Seismicity and tectonics of the South Shetland Islands and Bransfield Strait from a regional broadband seismograph deployment. Journal of Geophysical Research, 2003, 108, .	3.3	56
136	Seismological constraints on structure and flow patterns within the mantle wedge. Geophysical Monograph Series, 2003, , 59-81.	0.1	30
137	On the decompression melting structure at volcanic arcs and back-arc spreading centers. Geophysical Research Letters, 2002, 29, 17-1-17-4.	4.0	109
138	A teleseismic shear-wave splitting study to investigate mantle flow around South America and implications for plate-driving forces. Geophysical Journal International, 2002, 149, F1-F7.	2.4	33
139	Upper mantle discontinuity structure in the region of the Tonga Subduction Zone. Geophysical Research Letters, 2001, 28, 1855-1858.	4.0	29
140	Aftershock locations and rupture characteristics of the 1995 Mariana Deep Earthquake. Geophysical Research Letters, 2001, 28, 4311-4314.	4.0	9
141	Seismological constraints on the mechanism of deep earthquakes: temperature dependence of deep earthquake source properties. Physics of the Earth and Planetary Interiors, 2001, 127, 145-163.	1.9	111
142	A Complex Pattern of Mantle Flow in the Lau Backarc. Science, 2001, 292, 713-716.	12.6	248
143	Repeating Deep Earthquakes: Evidence for Fault Reactivation at Great Depth. Science, 2001, 293, 1463-1466.	12.6	44
144	Aftershocks of the March 9, 1994, Tonga earthquake: The strongest known deep aftershock sequence. Journal of Geophysical Research, 2000, 105, 19067-19083.	3.3	29

#	Article	IF	CITATIONS
145	An empirical relationship between seismic attenuation and velocity anomalies in the upper mantle. Geophysical Research Letters, 2000, 27, 601-604.	4.0	59
146	The waveguide effect of metastable olivine in slabs. Geophysical Research Letters, 2000, 27, 581-584.	4.0	21
147	Crust and upper mantle heterogeneities in the southwest Pacific from surface wave phase velocity analysis. Physics of the Earth and Planetary Interiors, 1999, 110, 211-234.	1.9	16
148	Seismic attenuation tomography of the Tonga-Fiji region using phase pair methods. Journal of Geophysical Research, 1999, 104, 4795-4809.	3.3	101
149	Depression of the 660 km discontinuity beneath the Tonga Slab determined from near-verticalScSreverberations. Geophysical Research Letters, 1999, 26, 1223-1226.	4.0	13
150	Constraints on the origin of slab and mantle wedge anomalies in Tonga from the ratio of StoPvelocities. Journal of Geophysical Research, 1999, 104, 15089-15104.	3.3	21
151	Anisotropy and Flow in Pacific Subduction Zone Back-arcs. Pure and Applied Geophysics, 1998, 151, 463-475.	1.9	70
152	Attenuation of Broadband P and S Waves in Tonga: Observations of Frequency Dependent Q. Pure and Applied Geophysics, 1998, 153, 345-375.	1.9	43
153	Source and aftershock properties of the 1996 Flores Sea Deep Earthquake. Geophysical Research Letters, 1998, 25, 781-784.	4.0	7
154	Correction to "Source and aftershock properties of the 1996 Flores Sea Deep Earthquake― Geophysical Research Letters, 1998, 25, 2011-2011.	4.0	0
155	Modeling the Tonga slab: Can travel time data resolve a metastable olivine wedge?. Journal of Geophysical Research, 1998, 103, 30079-30100.	3.3	55
156	GEOSCIENCE: Enhanced: Sliding Skis and Slipping Faults. Science, 1998, 279, 824-825.	12.6	4
157	Attenuation of Broadband P and S Waves in Tonga: Observations of Frequency Dependent Q. , 1998, , 345-375.		2
158	Anisotropy and Flow in Pacific Subduction Zone Back-arcs. , 1998, , 463-475.		0
159	Upper mantle structure of the southwest Pacific from regional waveform inversion. Journal of Geophysical Research, 1997, 102, 27439-27451.	3.3	39
160	State of stress before and after the 1994 Northridge Earthquake. Geophysical Research Letters, 1997, 24, 519-522.	4.0	54
161	Aftershock sequences of moderate-sized intermediate and deep earthquakes in the Tonga Subduction Zone. Geophysical Research Letters, 1997, 24, 2059-2062.	4.0	18
162	Depth Extent of the Lau Back-Arc Spreading Center and Its Relation to Subduction Processes. Science, 1997, 278, 254-257.	12.6	290

#	Article	IF	CITATIONS
163	The March 9, 1994 (Mw7.6), deep Tonga earthquake: Rupture outside the seismically active slab. Journal of Geophysical Research, 1997, 102, 15163-15182.	3.3	57
164	The Flinn-Engdahl Regionalisation Scheme: The 1995 revision. Physics of the Earth and Planetary Interiors, 1996, 96, 223-297.	1.9	66
165	The depth distribution of mantle anisotropy beneath the Tonga subduction zone. Earth and Planetary Science Letters, 1996, 142, 253-260.	4.4	115
166	Tomography of the Source Area of the 1995 Kobe Earthquake: Evidence for Fluids at the Hypocenter?. Science, 1996, 274, 1891-1894.	12.6	328
167	Effect of slab temperature on deep-earthquake aftershock productivity and magnitude–frequency relations. Nature, 1996, 384, 153-156.	27.8	74
168	The 1994 Bolivia and Tonga events: Fundamentally different types of deep earthquakes?. Geophysical Research Letters, 1995, 22, 2245-2248.	4.0	45
169	A double seismic zone in New Britain and the morphology of the Solomon Plate at intermediate depths. Geophysical Research Letters, 1995, 22, 1965-1968.	4.0	30
170	A deep earthquake aftershock sequence and implications for the rupture mechanism of deep earthquakes. Nature, 1994, 372, 540-543.	27.8	84
171	Radial upper mantle attenuation structure of inactive back arc basins from differential shear wave measurements. Journal of Geophysical Research, 1994, 99, 15469.	3.3	42
172	Too hot for earthquakes?. Nature, 1993, 363, 299-300.	27.8	12
173	Evidence for transformational faulting from a deep double seismic zone in Tonga. Nature, 1993, 364, 790-793.	27.8	96
174	Evidence from earthquakes for bookshelf faulting at large non-transform ridge offsets. Nature, 1993, 362, 235-237.	27.8	49
175	Tsunami earthquakes: Slow thrustâ€faulting events in the accretionary wedge. Journal of Geophysical Research, 1992, 97, 15321-15337.	3.3	158
176	Thermoelastic stress in oceanic lithosphere due to hotspot reheating. Journal of Geophysical Research, 1991, 96, 18323-18334.	3.3	8
177	A further proposal for additional regions for the Flinn-Engdahl Regionalization Scheme. Geophysical Journal International, 1990, 103, 759-762.	2.4	2
178	The November 20,1960 Peru Tsunami Earthquake: Source mechanism of a slow event. Geophysical Research Letters, 1990, 17, 661-664.	4.0	49
179	Attenuation structure beneath the Lau Back Arc Spreading Center from teleseismic <i>S</i> phases. Geophysical Research Letters, 1990, 17, 2117-2120.	4.0	36
180	The largest recorded earthquake swarm: Intraplate faulting near the Southwest Indian Ridge. Journal of Geophysical Research, 1990, 95, 4735-4750.	3.3	13

#	Article	IF	CITATIONS
181	Bathymetric effects on body waveforms from shallow subduction zone earthquakes and application to seismic processes in the Kurile Trench. Journal of Geophysical Research, 1989, 94, 2955-2972.	3.3	69
182	Seismotectonics and relative plate motions in the Scotia Sea region. Journal of Geophysical Research, 1989, 94, 7293-7320.	3.3	257
183	Historical seismicity and implications for diffuse plate convergence in the northeast Indian Ocean. Journal of Geophysical Research, 1989, 94, 12301-12319.	3.3	95
184	Rupture characteristics of the 1982 Tonga and 1986 Kermadec earthquakes. Journal of Geophysical Research, 1989, 94, 15521-15539.	3.3	21
185	A test of alternative Caribbean Plate relative motion models. Journal of Geophysical Research, 1988, 93, 3041-3050.	3.3	91
186	Seismic rupture associated with subduction of the Cocos Ridge. Tectonics, 1987, 6, 757-774.	2.8	46
187	Effects of near source bathymetry on teleseismic P waveforms. Geophysical Research Letters, 1987, 14, 761-764.	4.0	57
188	Tensional intraplate seismicity in the Eastcentral Pacific. Physics of the Earth and Planetary Interiors, 1987, 49, 264-282.	1.9	10
189	Why does near ridge extensional seismicity occur primarily in the Indian Ocean?. Earth and Planetary Science Letters, 1987, 82, 107-113.	4.4	15
190	Historical seismicity near Chagos: a complex deformation zone in the equatorial Indian Ocean. Earth and Planetary Science Letters, 1986, 76, 350-360.	4.4	61
191	Mechanisms and depths of Atlantic transform earthquakes. Journal of Geophysical Research, 1986, 91, 548-577.	3.3	144
192	Comment on "Subduction of aseismic ridges beneath the Caribbean Plate: Implications for the tectonics and seismic potential of the northeastern Caribbean―by W. R. McCann and L. R. Sykes. Journal of Geophysical Research, 1986, 91, 784-786.	3.3	15
193	The Nazcaâ€South America convergence rate and the recurrence of the Great 1960 Chilean Earthquake. Geophysical Research Letters, 1986, 13, 713-716.	4.0	35
194	Depth determination for shallow teleseismic earthquakes: Methods and results. Reviews of Geophysics, 1986, 24, 806-832.	23.0	72
195	Plate tectonic models for Indian Ocean "intraplate―deformation. Tectonophysics, 1986, 132, 37-48.	2.2	79
196	Implications of oceanic intraplate seismicity for plate stresses, driving forces and rheology. Tectonophysics, 1985, 116, 143-162.	2.2	108
197	A diffuse plate boundary model for Indian Ocean tectonics. Geophysical Research Letters, 1985, 12, 429-432.	4.0	205
198	Intraplate seismicity and stresses in young oceanic lithosphere. Journal of Geophysical Research, 1984, 89, 11442-11464.	3.3	189

#	Article	IF	CITATIONS
199	Impaired Brain Functions Due to Diazepam and Meprobamate Abuse in a 53-Year-Old-Male. Journal of Nervous and Mental Disease, 1984, 172, 498-501.	1.0	4
200	Slow subduction of old lithosphere in the lesser antilles. Tectonophysics, 1983, 99, 139-148.	2.2	18
201	Age dependence of oceanic intraplate seismicity and implications for lithospheric evolution. Journal of Geophysical Research, 1983, 88, 6455-6468.	3.3	320
202	The 1966 Kremasta reservoir earthquake sequence. Earth and Planetary Science Letters, 1982, 59, 49-60.	4.4	23
203	Subduction seismicity and tectonics in the Lesser Antilles Arc. Journal of Geophysical Research, 1982, 87, 8642-8664.	3.3	109
204	Seismological Constraints on Earth's Deep Water Cycle. Geophysical Monograph Series, 0, , 13-27.	0.1	8